РАДІАЦІЙНА ФІЗИКА
RADIATION PHYSICS

УДК 621.039.58 https://doi.org/10.15407/jnpae2023.01.040

M. Aygun[1], Z. Aygun[2,*]

[1] *Bitlis Eren University, Science and Art Faculty, Physics Department, Bitlis, Turkey*
[2] *Bitlis Eren University, Vocational School of Technical Sciences, Bitlis, Turkey*

*Corresponding author: zeynep.yarbasi@gmail.com

DENSITY-DEPENDENT ANALYTICAL EQUATIONS OF RADIATION SHIELDING PARAMETERS FOR SUPER ALLOYS BY LINEAR REGRESSION ANALYSIS

Super alloys have great interest with good mechanical strength, surface stability, high operating temperatures, and high resistance to corrosion and oxidation features. In the study, new, reliable, and practical equations which give the radiation shielding parameters depending on the density of super alloys are obtained. For this analysis, MAR-247, MAR-302, Inconel 625, Inconel 718, Nimocast 75, WI-52, Inconel 617, Incoloy 800HT, Inconel 939, 713LC, and 7925A super alloys are chosen. The radiation shielding parameters such as linear attenuation coefficient, effective atomic number, half value layer, mean free path, and fast neutron removal cross-section are calculated by using Phy-X/PSD program. Then, new analytical equations providing the radiation shielding parameters by linear regression analysis are evaluated.

Keywords: super alloy, linear regression analysis, radiation shielding parameters, density-dependent analytical equations.

1. Introduction

As a result of the increase in radiological and nuclear technology applications, exposure to radiation in many periods of our lives is now an inevitable reality. For this reason, it is essential to take measures to reduce the harmful effects of both natural and human-induced radiation, although it cannot be completely prevented. Every day, scientists are interested in producing new and non-toxic materials for this purpose. Alloy is the material obtained by mixing a metal element with at least one element (metal or nonmetal) in certain proportions. This new material still has a metal character. It is essential to use alloys with the required properties in cases where pure metals are insufficient for all kinds of effects such as high temperatures, corrosion, chemical effects, etc. Alloys can be classified according to their applications, contents, or base metals. Base metals can include nickel, lead, tungsten, cobalt, copper, iron, etc. Alloys with different bases and contents are searched widely for radiation shielding purposes due to their various superior features [1 - 5]. Super alloys are important materials with main features such as high strength, resistance to thermal creep deformation, good surface stability, and high resistance to corrosion or oxidation at high temperatures. These properties make super alloys favorable for also radiation protection applications. In this respect, many studies have been carried out to determine the radiation shielding abilities of super alloys before [6 - 9].

The high atomic number and high density of materials are important for their efficiency as a radiation shield. The efficiency of a radiation shielding material can be defined by determining radiation attenuation parameters such as linear attenuation coefficient (LAC), effective atomic number (Z_{eff}), half value layer (HVL), mean free path (MFP), and fast neutron removal cross-section (FNRCS). HVL is the thickness-related parameter used in choosing any radiation protection material by halving the photon intensity. MFP is the distance taken by radiation between subsequent collisions in the matter. Lower values of HVL and MFP are preferred for higher shielding potential. LAC relates to the material's ability to absorb photons per unit thickness and depends on both the density and mass attenuation coefficient of the sample. Z_{eff} is the average atomic number affected by the atomic numbers of the constituent atoms in the composition. FNRCS can be defined as the capability of the material to attenuate fast neutrons. The common feature of the parameters mentioned above is depending on density.

The aim of this study is to evaluate the dependency of LAC, Z_{eff}, MFP, HVL, and FNRCS values of nickel and cobalt based super alloys (MAR-247, MAR-302, Inconel 625, Inconel 718, Nimocast 75, WI-52, Inconel 617, Incoloy 800HT, Inconel 939, 713LC and 7925A) on density. For the purpose of this evaluation, the parameters are calculated by Phy-X/PSD code developed by Sakar et al. [10]. The variation of results of the super alloys with density for different photon energies is expressed by linear regression equations with the coefficient of

determination (CD). Regression analysis, one of the traditional methods, is a statistical process that can help in developing an equation for faster and simpler prediction. It helps to model the relationship between one or more independent variables and one dependent variable by fitting a linear equation for the analyzed data [11, 12]. Linear regression is one of the numeric output estimation methods. The relationship between response (dependent) variables and explanatory (independent) variables can be modelled using linear regression. Linear regression, widely preferred for predictive analysis and modelling, is the process of finding a line that best fits the available data points in the graph. Thus, it can be used to predict output values for inputs that are absent in the data set [13, 14]. The linear regression method is used in medicine, radiation, construction, and building materials research to verify data or produce a mathematical formula to connect different variables together [11 - 18]. Laksminarayana et al. [15] studied the Gaussian curve fittings of the Raman spectra for the A–I glass with good accuracy by linear regression. The linear regression method associated with R^2 values was used to calculate the LAC (μ) of concrete samples by Zayed et al. [16]. An exponential linear relationship was obtained between the γ-ray fluxes and thicknesses for concrete mixes. Elsayed et al. [11] investigated the effects of adding different nano additives (Nano alumina, Carbon Nanotubes, etc.) within normal strength concrete and used the linear regression method for developing an empirical equation for the prediction of residual compressive strength and LAC. Relation between the factors: of age, underlying health conditions, population density, and temperature with the death rate of COVID-19 was studied by regression models including linear regression [17]. The dependence of the LAC, Z_{eff}, and HVL of Rene alloys on density were evaluated by linear regression in a previous study by Aygun and Aygun [18].

2. Methods

The quality of linear regression can be measured by the CD, or R^2, and calculated as [15],

$$R^2 = 1 - \frac{\text{Sum of squares of residuals}}{\text{Sum of squares of predicted values}},$$

where sum of squares of residual (*RSS*) is the sum of the squares of the vertical deviations (y_i), e_i, from each data point (x_i) to the fitted line:

$$RSS = \sum_{i=1}^{n} e_i = \sum_{i=1}^{n} w_i \left(y_i - y_{ave} \right)^2$$

with w_i is the instrumental weighting ($w_i = 1/\sigma_i^2$), σ_i is the measurement uncertainty.

While sum of squares of predicted values (*TSS*) is the total sum of squares of vertical deviations:

$$TSS = \sum_{i=1}^{n} \left(y_i - y_{ave} \right)^2 .$$

In the study, the chemical compositions of the super alloys were taken from the literature [7, 9, 19, 20] and given in Table 1. The density (ρ_{mix}) of alloys is determined by the rule of the mixture as follows [21]:

$$\rho_{mix} = \frac{\sum_{i=1}^{n} c_i A_i}{\sum_{i=1}^{n} c_i A_i / \rho_i}, \qquad (1)$$

where ρ_i, c_i, and A_i are the density, atomic fraction, and atomic weight of element i_{th}, respectively.

Information on the parameters and the formulas are explained in detail in previous studies [8, 10, 22] and also are given in Table 2.

Table 1. **Chemical compositions (wt%) and densities of the super alloys**

Element	In617	In800HT	In939	713LC	7925A	In718	In625	MAR-247	MAR-302	Nim75	WI-52
Ta	–	–	–	–	4.120	–	–	3.000	9.000	–	–
Zr	–	–	–	0.010	0.031	–	–	0.040	–	–	–
Nb	–	–	1.010	1.960	0.100	5.100	3.600	–	–	–	–
W	–	–	2.000	–	4.100	–	–	10.00	10.00	-	11.00
C	0.080	0.061	0.150	0.050	0.078	–	–	0.020	0.850	0.120	0.850
Mn	0.230	1.270	–	–	–	–	–	–	–	–	–
Fe	1.460	46.24	–	0.190	0.160	18.50	2.000	–	1.500	–	2.000
S	0.001	0.001	–	–	–	–	–	–	–	–	–
Si	0.200	0.420	–	–	–	–	–	–	–	–	–
Cu	0.020	0.200	–	–	–	–	–	–	–	–	–
Ni	53.27	30.65	48.80	74.77	61.10	52.50	61.00	59.63	–	79.88	1.000
Cr	22.02	19.70	22.80	11.90	12.28	19.00	21.50	8.500	21.50	20.00	21.50
Al	1.100	0.560	1.440	5.750	3.360	0.500	0.200	5.600	–	–	–
Ti	0.320	0.540	4.100	0.700	3.980	0.900	0.200	1.000	0.200	–	–

Continuation of Table 1

Element	In617	In800HT	In939	713LC	7925A	In718	In625	MAR-247	MAR-302	Nim75	WI-52
Co	11.91	0.100	19.70	0.080	8.870	–	–	10.00	56.94	–	63.65
Mo	9.380	–	–	4.570	1.810	3.000	9.000	0.650	–	–	–
P	0.005	0.024	–	–	–	–	–	–	–	–	–
B	0.002	–	–	0.013	0.015	–	–	0.020	0.010	–	–
Hf	–	–	–	–	–	–	–	1.400	–	–	–
Density	8.360	7.940	8.380	8.210	9.210	8.220	8.440	8.530	9.210	8.440	8.880

Table 2. **Formulas of radiation shielding parameters**

Parameter	Formula	Unit	Symbols
LAC	$\mu = \rho\mu_m$	cm^{-1}	ρ - density of the material; μ_m - mass attenuation coefficient; μ - LAC
HVL	$In(2)/\mu$	cm	μ - LAC
MFP	$1/\mu$	cm	μ - LAC
Z_{eff}	σ_a/σ_e	–	σ_a - total atomic cross-section of material; σ_e - total electronic cross-section of material
FNRCS	$\sum R = \sum_i \rho_i \left(\sum R/\rho\right)_i$	cm^{-1}	$\left(\sum R/\rho\right)_i$ - mass removal cross-section of the i_{th} constituent element; ρ_i - partial density of the material

To determine shielding parameters, Phy-X/PSD program was used. The code which is available and applicable for all materials with density and composition in a wide energy range is preferred widely by researchers recently [4, 7, 8, 23, 24].

3. Result and discussion

The radiation shielding parameters were investigated for eleven various super alloys (713LC, 7925A, In800HT, In625, In718, In939, In617, MAR-247, MAR-302, Nimocast 75, and WI-52) at photon energies in the range from 1 keV to 100 GeV. The theoretical calculations were performed by using the Phy-X/PSD program.

In our study, firstly the LAC values were calculated by using the Phy-X/PSD program for 11 different super alloys. In this context, we performed 26 different calculations based on the linear regression method. Then, the analytical equations obtained as a result of these calculations are given in Table 3.

Table 3. **Analytical equations of LAC values at different energies for 11 different alloys by linear regression method**

Energy, MeV	Density-dependent analytical equation	R^2
0.015	$LAC = -733.00352 + 149.94634 \cdot \rho_{superalloy}$	0.76176
0.02	$LAC = -170.25792 + 51.44597 \cdot \rho_{superalloy}$	0.51049
0.03	$LAC = -63.86005 + 17.7349 \cdot \rho_{superalloy}$	0.48261
0.04	$LAC = -32.62392 + 8.42535 \cdot \rho_{superalloy}$	0.49339
0.05	$LAC = -19.43409 + 4.77172 \cdot \rho_{superalloy}$	0.51346
0.06	$LAC = -12.71694 + 3.02246 \cdot \rho_{superalloy}$	0.53789
0.08	$LAC = -65.60244 + 8.74656 \cdot \rho_{superalloy}$	0.64392
0.1	$LAC = -37.07021 + 4.97403 \cdot \rho_{superalloy}$	0.64608
0.15	$LAC = -12.64022 + 1.76456 \cdot \rho_{superalloy}$	0.66330
0.2	$LAC = -5.80514 + 0.86623 \cdot \rho_{superalloy}$	0.69214
0.3	$LAC = -1.91292 + 0.34754 \cdot \rho_{superalloy}$	0.76710
0.4	$LAC = -0.85472 + 0.20053 \cdot \rho_{superalloy}$	0.83883
0.5	$LAC = -0.44584 + 0.13998 \cdot \rho_{superalloy}$	0.89036
0.6	$LAC = -0.25176 + 0.1088 \cdot \rho_{superalloy}$	0.92121
0.8	$LAC = -0.08546 + 0.0781 \cdot \rho_{superalloy}$	0.94390
1	$LAC = -0.02074 + 0.063 \cdot \rho_{superalloy}$	0.94450
1.5	$LAC = 0.01988 + 0.04678 \cdot \rho_{superalloy}$	0.93488
2	$LAC = 0.01279 + 0.04146 \cdot \rho_{superalloy}$	0.93790
3	$LAC = -0.01445 + 0.03843 \cdot \rho_{superalloy}$	0.94823

Continuation of Table 3

Energy, MeV	Density-dependent analytical equation	R^2
4	$LAC = -0.03828 + 0.03832 \cdot \rho_{superalloy}$	0.95007
5	$LAC = -0.05791 + 0.03915 \cdot \rho_{superalloy}$	0.94660
6	$LAC = -0.07414 + 0.04031 \cdot \rho_{superalloy}$	0.94115
15	$LAC = -0.16535 + 0.05229 \cdot \rho_{superalloy}$	0.90275
150	$LAC = -0.3563 + 0.0917 \cdot \rho_{superalloy}$	0.87182
1500	$LAC = -0.41585 + 0.10735 \cdot \rho_{superalloy}$	0.87339
15000	$LAC = -0.42631 + 0.11033 \cdot \rho_{superalloy}$	0.87403

Table 4. **Analytical equations of Z_{eff} values at different energies for 11 different alloys by linear regression method**

Energy, MeV	Density-dependent analytical equation	R^2
0.015	$Z_{eff} = -14.30581 + 5.08288 \cdot \rho_{superalloy}$	0.58738
0.02	$Z_{eff} = -8.85668 + 4.5401 \cdot \rho_{superalloy}$	0.52338
0.03	$Z_{eff} = -11.29705 + 4.85219 \cdot \rho_{superalloy}$	0.52508
0.04	$Z_{eff} = -13.21699 + 5.09121 \cdot \rho_{superalloy}$	0.53064
0.05	$Z_{eff} = -14.42546 + 5.23797 \cdot \rho_{superalloy}$	0.53579
0.06	$Z_{eff} = -14.99563 + 5.30262 \cdot \rho_{superalloy}$	0.54047
0.08	$Z_{eff} = -113.06138 + 17.32998 \cdot \rho_{superalloy}$	0.62196
0.1	$Z_{eff} = -105.75744 + 16.40704 \cdot \rho_{superalloy}$	0.62092
0.15	$Z_{eff} = -75.90523 + 12.67924 \cdot \rho_{superalloy}$	0.61571
0.2	$Z_{eff} = -48.74001 + 9.30576 \cdot \rho_{superalloy}$	0.61249
0.3	$Z_{eff} = -17.3383 + 5.41925 \cdot \rho_{superalloy}$	0.61032
0.4	$Z_{eff} = -3.49535 + 3.70947 \cdot \rho_{superalloy}$	0.60107
0.5	$Z_{eff} = 3.28609 + 2.87256 \cdot \rho_{superalloy}$	0.58190
0.6	$Z_{eff} = 7.04627 + 2.40872 \cdot \rho_{superalloy}$	0.55777
0.8	$Z_{eff} = 10.82571 + 1.94267 \cdot \rho_{superalloy}$	0.51168
1	$Z_{eff} = 12.62471 + 1.72086 \cdot \rho_{superalloy}$	0.47645
1.5	$Z_{eff} = 14.06674 + 1.54353 \cdot \rho_{superalloy}$	0.43908
2	$Z_{eff} = 13.74225 + 1.58494 \cdot \rho_{superalloy}$	0.44858
3	$Z_{eff} = 12.05881 + 1.79672 \cdot \rho_{superalloy}$	0.48907
4	$Z_{eff} = 10.22231 + 2.02769 \cdot \rho_{superalloy}$	0.52090
5	$Z_{eff} = 8.57236 + 2.2353 \cdot \rho_{superalloy}$	0.54137
6	$Z_{eff} = 7.15228 + 2.41409 \cdot \rho_{superalloy}$	0.55452
15	$Z_{eff} = 0.2462 + 3.28366 \cdot \rho_{superalloy}$	0.58432
150	$Z_{eff} = -5.31548 + 3.98411 \cdot \rho_{superalloy}$	0.59024
1500	$Z_{eff} = -5.23097 + 3.97381 \cdot \rho_{superalloy}$	0.58961
15000	$Z_{eff} = -5.14908 + 3.96352 \cdot \rho_{superalloy}$	0.58945

Additionally, the LAC values were plotted as a function of densities of the super alloys at 0.015, 0.15, 1.5, 15, 150, and 1500 MeV photon energies in Fig. 1. The energy ranges evaluated in the analytical calculations are determined according to the changes in the LAC values by means of the Phy-X/PSD program. The energies where the difference between the LAC values is small were selected and analytical expressions were calculated for these energies. It is observed that the LAC values increase with the increase in densities of the super alloys. Also, it can be said that the variation of Phy-X/PSD results of the super alloys according to density for different photon energies can be expressed by linear regression equations with a good CD.

Then, the Z_{eff} values were calculated by using the Phy-X/PSD program for 11 different super alloys. The analytical equations determined for these values of the Z_{eff} are listed in Table 4. Additionally, the Z_{eff} values are displayed as a function of densities of the super alloys at 0.015, 0.15, 1.5, 15, 150, and 1500 MeV in Fig. 2. The energy values were determined as LAC values. It is noticed that the Z_{eff} values increase with the increase in densities of the super alloys. Also, it can be expressed that the analytical equations of the super alloys introduced according to density for different photon energies have average values of CD.

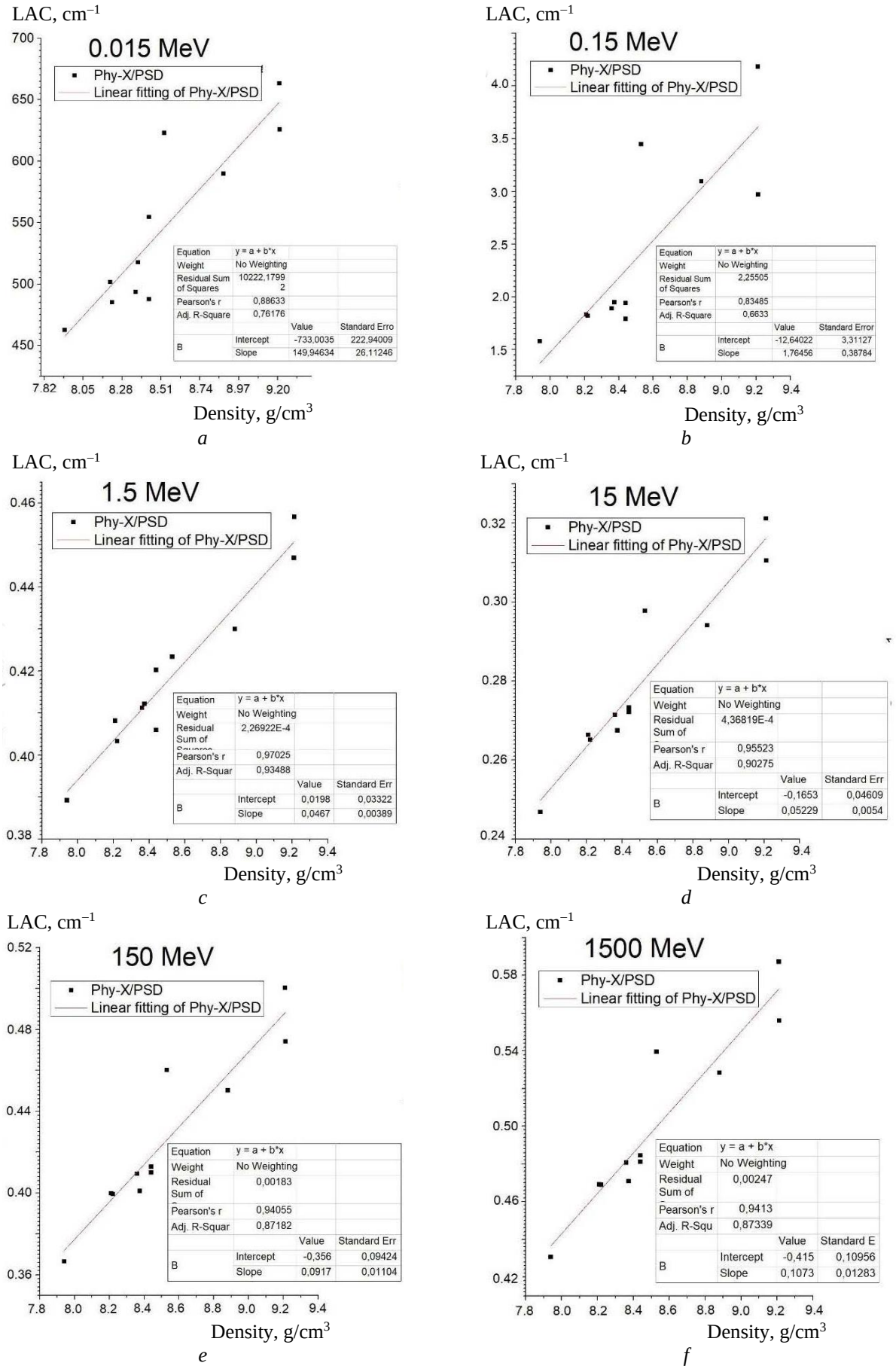

Fig. 1. The LAC values as a function of densities of the super alloys at 0.015, 0.15, 1.5, 15, 150, and 1500 MeV photon energies.

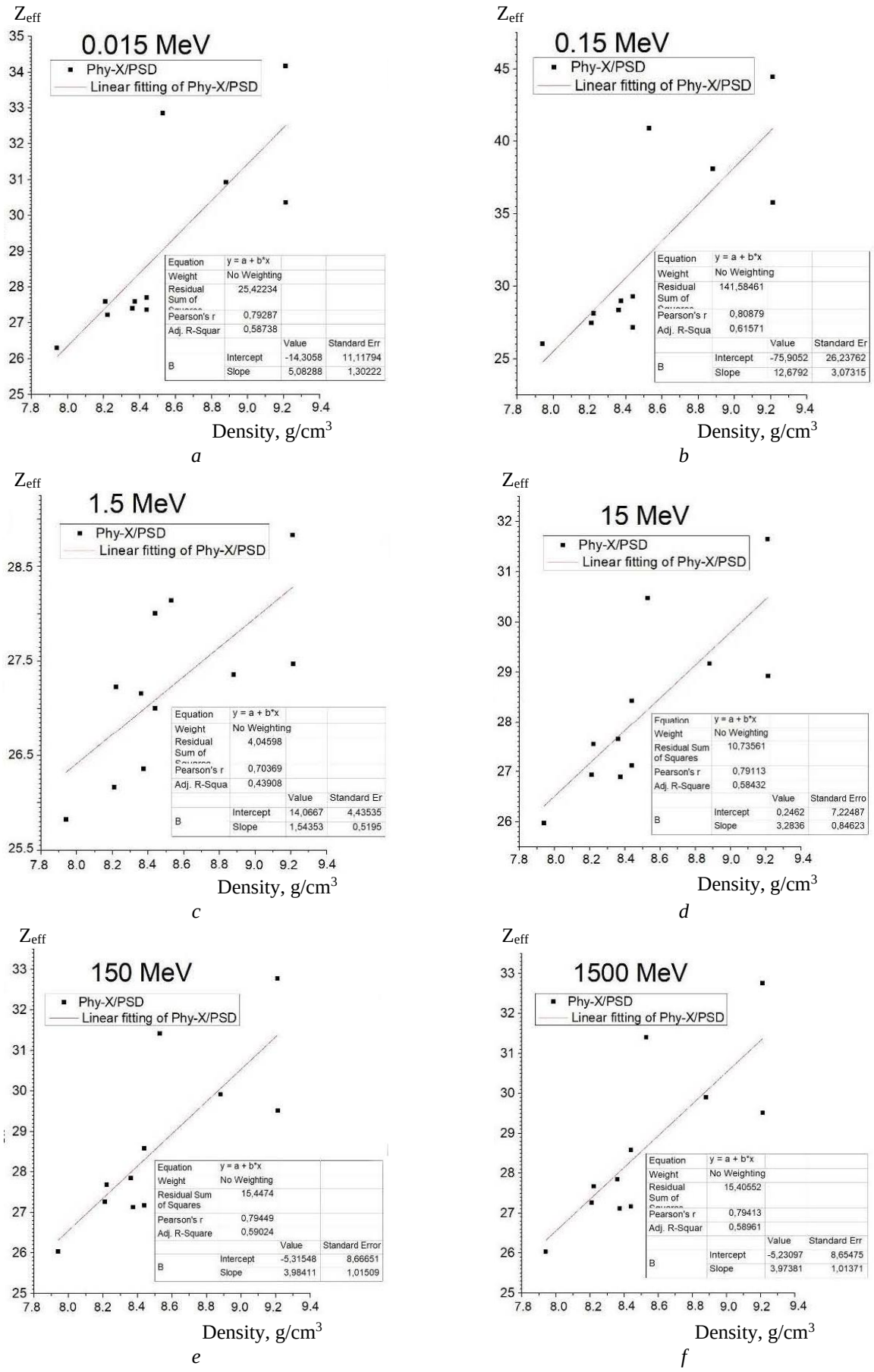

Fig. 2. The Z_{eff} values as a function of densities of the super alloys at 0.015, 0.15, 1.5, 15, 150, and 1500 MeV photon energies.

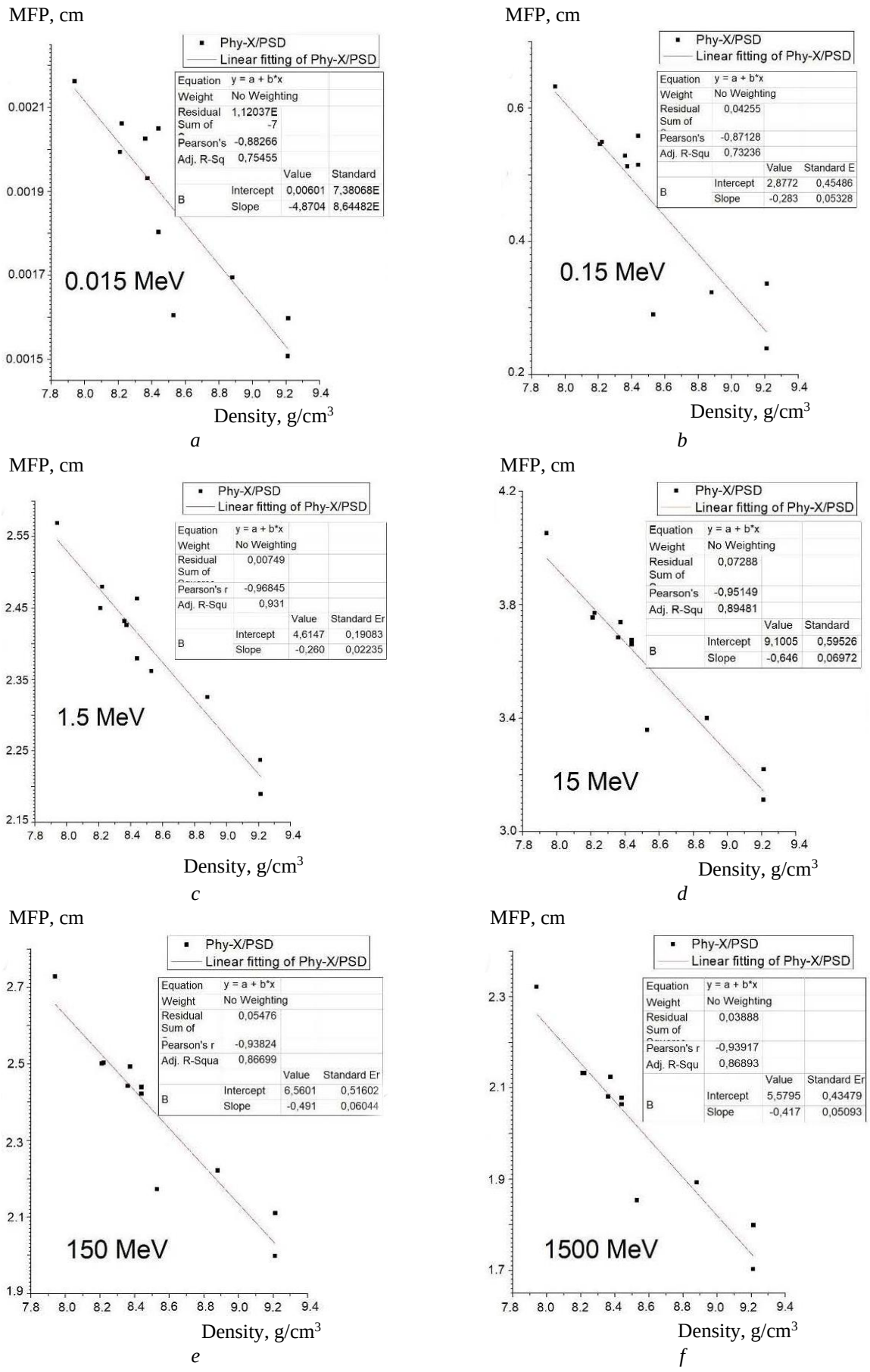

Fig. 3. The MFP values as a function of densities of the super alloys at 0.015, 0.15, 1.5, 15, 150, and 1500 MeV photon energies.

Table 5. **Analytical equations of MFP values at different energies for 11 different alloys by linear regression method**

Energy, MeV	Density-dependent analytical equation	R^2
0.015	MFP = 0.00601 – 0.000487046 · $\rho_{superalloy}$	0.75455
0.02	MFP = 0.01029 – 0.000765452 · $\rho_{superalloy}$	0.46351
0.03	MFP = 0.03305 – 0.00252 · $\rho_{superalloy}$	0.43917
0.04	MFP = 0.07641 – 0.00593 · $\rho_{superalloy}$	0.44762
0.05	MFP = 0.1448 – 0.01138 · $\rho_{superalloy}$	0.46444
0.06	MFP = 0.23946 – 0.01896 · $\rho_{superalloy}$	0.48600
0.08	MFP = 1.03655 – 0.10605 · $\rho_{superalloy}$	0.72845
0.1	MFP = 1.65015 – 0.16786 · $\rho_{superalloy}$	0.72921
0.15	MFP = 2.87727 – 0.28374 · $\rho_{superalloy}$	0.73236
0.2	MFP = 3.39503 – 0.31987 · $\rho_{superalloy}$	0.74318
0.3	MFP = 3.49034 – 0.29555 · $\rho_{superalloy}$	0.79069
0.4	MFP = 3.41032 – 0.26154 · $\rho_{superalloy}$	0.84661
0.5	MFP = 3.4002 – 0.24104 · $\rho_{superalloy}$	0.88980
0.6	MFP = 3.4506 – 0.23048 · $\rho_{superalloy}$	0.91673
0.8	MFP = 3.65039 – 0.22551 · $\rho_{superalloy}$	0.93767
1	MFP = 3.90515 – 0.23036 · $\rho_{superalloy}$	0.93897
1.5	MFP = 4.61476 – 0.26059 · $\rho_{superalloy}$	0.93100
2	MFP = 5.30996 – 0.30191 · $\rho_{superalloy}$	0.93347
3	MFP = 6.46297 – 0.38263 · $\rho_{superalloy}$	0.94144
4	MFP = 7.30925 – 0.44956 · $\rho_{superalloy}$	0.94176
5	MFP = 7.91464 – 0.50183 · $\rho_{superalloy}$	0.93747
6	MFP = 8.33457 – 0.54095 · $\rho_{superalloy}$	0.93171
15	MFP = 9.10059 – 0.64682 · $\rho_{superalloy}$	0.89481
150	MFP = 6.56019 – 0.4917 · $\rho_{superalloy}$	0.86699
1500	MFP = 5.5795 – 0.41776 · $\rho_{superalloy}$	0.86893
15000	MFP = 5.40967 – 0.40472 · $\rho_{superalloy}$	0.86966

Table 6. **Analytical equations of HVL values at different energies for 11 different alloys by linear regression method**

Energy, MeV	Density-dependent analytical equation	R^2
0.015	HVL = 0.00417 – 0.000337594 · $\rho_{superalloy}$	0.75455
0.02	HVL = 0.00713 – 0.000530571 · $\rho_{superalloy}$	0.46351
0.03	HVL = 0.02291 – 0.00174 · $\rho_{superalloy}$	0.43917
0.04	HVL = 0.05297 – 0.00411 · $\rho_{superalloy}$	0.44762
0.05	HVL = 0.10036 – 0.00789 · $\rho_{superalloy}$	0.46444
0.06	HVL = 0.16598 – 0.01314 · $\rho_{superalloy}$	0.48600
0.08	HVL = 0.71848 – 0.07351 · $\rho_{superalloy}$	0.72845
0.1	HVL = 1.1438 – 0.11635 · $\rho_{superalloy}$	0.72921
0.15	HVL = 1.99437 – 0.19667 · $\rho_{superalloy}$	0.73236
0.2	HVL = 2.35325 – 0.22172 · $\rho_{superalloy}$	0.74318
0.3	HVL = 2.41932 – 0.20486 · $\rho_{superalloy}$	0.79069
0.4	HVL = 2.36386 – 0.18129 · $\rho_{superalloy}$	0.84661
0.5	HVL = 2.35684 – 0.16707 · $\rho_{superalloy}$	0.88980
0.6	HVL = 2.39178 – 0.15976 · $\rho_{superalloy}$	0.91673
0.8	HVL = 2.53026 – 0.15631 · $\rho_{superalloy}$	0.93767
1	HVL = 2.70685 – 0.15967 · $\rho_{superalloy}$	0.93897
1.5	HVL = 3.19871 – 0.18063 · $\rho_{superalloy}$	0.93100
2	HVL = 3.68058 – 0.20927 · $\rho_{superalloy}$	0.93347
3	HVL = 4.47979 – 0.26522 · $\rho_{superalloy}$	0.94144
4	HVL = 5.06639 – 0.31161 · $\rho_{superalloy}$	0.94176
5	HVL = 5.48601 – 0.34784 · $\rho_{superalloy}$	0.93747
6	HVL = 5.77708 – 0.37496 · $\rho_{superalloy}$	0.93171
15	HVL = 6.30805 – 0.44834 · $\rho_{superalloy}$	0.89481
150	HVL = 4.54718 – 0.34082 · $\rho_{superalloy}$	0.86699
1500	HVL = 3.86742 – 0.28957 · $\rho_{superalloy}$	0.86893
15000	HVL = 3.7497 – 0.28053 · $\rho_{superalloy}$	0.86966

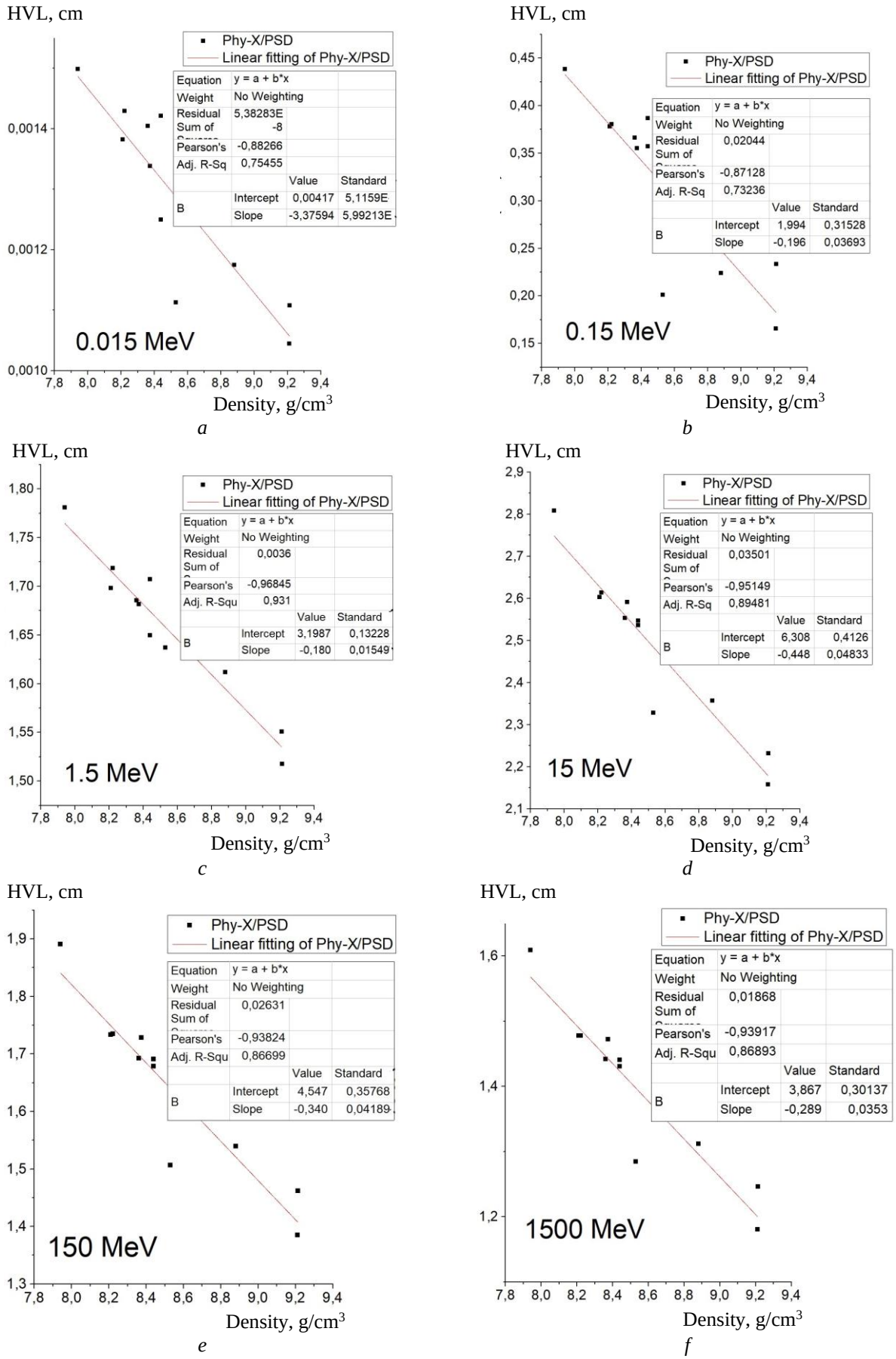

Fig. 4. The HVL values as a function of densities of the super alloys at 0.015, 0.15, 1.5, 15, 150, and 1500 MeV photon energies.

The analytical equations for MFP values calculated by using the Phy-X/PSD program for 11 different super alloys are presented in Table 5. The MFP values are plotted as a function of density for 0.015, 0.15, 1.5, 15, 150, and 1500 MeV photon energies in Fig. 3. It is observed that the MFP values decreased with an increase in densities of the super alloys. It can be said that the analytical equations can give agreement results according to the density at mid and higher photon energies.

In our study, the HVL values were calculated by using the program for 11 various super alloys. The analytical equations for the theoretical calculations are listed in Table 6. Also, the HVL values as a function of densities of the super alloys are shown at 0.015, 0.15, 1.5, 15, 150, and 1500 MeV in Fig. 4. It is noticed that the HVL values decrease with an increase in densities of the super alloys. Additionally, it can be said that the analytical equations expressed by linear regression equations are in good agreement with a good CD at mid and higher energies.

Finally, the fast neutron attenuation abilities of the alloys were also determined by Phy-X/PSD. The analytical equation for the theoretical calculation of FNRCS is given by

$$\text{FNRCS} = 0.07699 + 0.01017 \cdot \rho_{\text{Superalloy}}. \quad (2)$$

It is obtained that the FNRCS values increase with the increase in densities of the super alloys (Fig. 5).

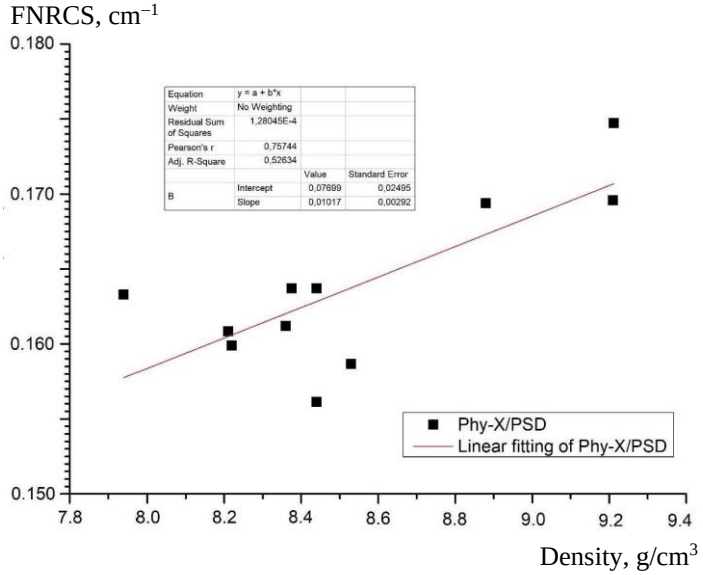

Fig. 5. The FNRCS values as a function of the densities of the super alloys.

4. Conclusion

In the present study, new, practical, and valid equations on radiation shielding parameters of eleven various super alloys such as 713LC, 7925A, 800HT, In625, In718, In939, In617, MAR-247, MAR-302, Nimocast 75, and WI-52 have been researched. The linear regression method has been applied to obtain the LAC, Z_{eff}, MFP, HVL, and FNRCS parameters of some important super alloys at 15 keV - 15 GeV. The analytical equations are given for the first time as a function of the density in tables and graphically presented for low, medium, and high energy values for each parameter in the figures. Generally, the calculated R^2 values for super alloys make it possible to conclude that the obtained regression equations are in good agreement with a good CD at mid and higher energies than those at low energies. Thus, the LAC, Z_{eff}, MFP, HVL, and FNRCS values can be determined without making very complex calculations according to the density distribution at different energies with the help of analytical expressions obtained for super alloys. It can be said that the application of this method over different composites and energies will be very reliable and practical. We are not too ambitious for definitive results here. Our aim with this study is to develop a different approach in the calculation of some parameters. Based on the results of this approach, important contributions can be made to theoretical studies by different methods.

REFERENCES

1. M.H.A. Mhareb et al. Radiation shielding features for various tellurium-based alloys: a comparative study. J. Mater. Sci.: Mater. Electron. 32 (2021) 26798.
2. H.C. Manjunatha et al. A study of X-ray, gamma and neutron shielding parameters in Si-alloys. Radiat. Phys. Chem. 165 (2019) 108414.
3. A.H. Almuqrin et al. Radiation shielding properties of selected alloys using EPICS2017 data library. Progress Nucl. Energy 137 (2021) 103748.

4. Z. Aygun, M. Aygun. A Theoretical Study on Radiation Shielding Characteristics of Magnetic Shielding Alloys, $Ni_{80}Fe_{15}Mo_5$ and $Ni_{77}Fe_{14}Cu_5Mo_4$, by Determining the Photon Attenuation Parameters in the Energy Range of 15keV-100GeV. Karaelmas Sci. Engineer. J. 11(2) (2021) 165.
5. A.M. Reda, A.A. El-Daly, E.A. Eid. Neutron/gamma radiation shielding characteristics and physical properties of (97.3−x)Pb−xCd–2.7Ag alloys for nuclear radiation applications. Phys. Scr. 96 (2021) 125321.
6. F.I. El-Agawany et al. Gamma-ray shielding capacity of different B4C-, Re-, and Ni-based superalloys. Eur. Phys. J. Plus 136 (2021) 527.
7. Z. Aygun, M. Aygun. Evaluation of radiation shielding potentials of Ni-based alloys, Inconel-617 and Incoloy-800HT, candidates for high temperature applications especially for nuclear reactors, by EpiXS and Phy-X/PSD codes. J. Polytech. (2022). In press.
8. N. Ekinci et al. Synthesis, physical properties, and gamma-ray shielding capacity of different Ni-based super alloys. Radiation Physics and Chemistry 186 (2021) 109483.
9. M.I. Sayyed et al. Evaluation of Radiation Shielding Features of Co and Ni-Based Superalloys Using MCNP-5 Code: Potential Use in Nuclear Safety. Appl. Sci. 10 (2020) 7680.
10. E. Şakar et al. Phy-X / PSD: Development of a user friendly online software for calculation of parameters relevant to radiation shielding and dosimetry. Radiat. Phys. Chem. 166 (2020) 108496.
11. A.A. El-Sayed et al. Using artificial neural networks for predicting mechanical and radiation shielding properties of different nano-concretes exposed to elevated temperature. Const. Building Mater. 324 (2022) 126663.
12. S. Chithra et al. A comparative study on the compressive strength prediction models for High Performance Concrete containing nano silica and copper slag using regression analysis and Artificial Neural Networks. Const. Building Mater. 114 (2016) 528.
13. J.-S. Chou, C.-F. Tsai. Concrete compressive strength analysis using a combined classification and regression technique. Autom. Constr. 24 (2012) 52.
14. M.H. Kutner et al. *Applied Linear Regression Models*. 4th ed. (McGraw Hill, 2004) 701 p.
15. G. Lakshminarayana et al. Investigation of structural, thermal properties and shielding parameters for multicomponent borate glasses for gamma and neutron radiation shielding applications. J. Non-Cryst. Solids 471 (2017) 222.
16. A.M. Zayed et al. Influence of heavyweight aggregates on the physico-mechanical and radiation attenuation properties of serpentine-based concrete. Const. Building Mater. 260 (2020) 120473.
17. C.D. Kudupudi et al. Identifying Correlation of Multiple Factors with Mortality Rate of COVID-19 Using Regression Models. Proc. of the Northeast Business & Economics Association (2020) p. 89.
18. Z. Aygun, M. Aygun. Radiation Shielding Potentials of Rene Alloys by Phy-X/PSD Code. Acta Physica Polonica A 141 (2022) 507.
19. M. Petrenec, K. Obrtlík, J. Polák. High Temperature Low Cycle Fatigue of Superalloys Inconel 713LC and Inconel 792-5A. Key Engineer. Mater. 348-349 (2007) 101.
20. A. Formenti, A. Eliasson, H. Fredriksson. On the Dendritic Growth and Microsegregation in Ni-Base Superalloys In718, In625 and In939. High Temperature Mater. Processes 24(4) (2005) 221.
21. C. Xiang et al. Design of single-phase high-entropy alloys composed of low thermal neutron absorption cross-section elements for nuclear power plant application. Intermetallics 104 (2019) 143.
22. E. Şakar. Determination of photon-shielding features and build-up factors of nickel-silver alloys. Radiat. Phys. Chem. 172 (2020) 108778.
23. B. Alim. Determination of Radiation Protection Features of the Ag_2O Doped Boro-Tellurite Glasses Using Phy-X / PSD Software. J. Inst. Sci. Tech. 10(1) (2020) 202.
24. I. Akkurt, H.O. Tekin. Radiological parameters of bismuth oxide glasses using the Phy-X/PSD software. Emerging Mater. Res. 9(3) (2020) 1020.

М. Айгюн[1], З. Айгюн[2,*]

[1] Університет Бітліс Ерен, Факультет науки і мистецтв, Кафедра фізики, Бітліс, Туреччина
[2] Університет Бітліс Ерен, Професійно-технічний ліцей, Бітліс, Туреччина

*Відповідальний автор: zeynep.yarbasi@gmail.com

АНАЛІТИЧНІ РІВНЯННЯ ДЛЯ ПАРАМЕТРІВ РАДІАЦІЙНОГО ЗАХИСТУ ДЛЯ СУПЕРСПЛАВІВ, ЗАЛЕЖНІ ВІД ГУСТИНИ, З ЛІНІЙНИМ РЕГРЕСІЙНИМ АНАЛІЗОМ

Суперсплави викликають великий інтерес завдяки хорошій механічній міцності, стабільності поверхні, високим робочим температурам і високій опірності до корозії та окисленню. У дослідженні отримано нові надійні та практичні рівняння, що дають параметри радіаційного захисту залежно від щільності суперсплавів. Для цього аналізу обрано суперсплави MAR-247, MAR-302, Inconel 625, Inconel 718, Nimocast 75, WI-52, Inconel 617, Incoloy 800HT, Inconel 939, 713LC і 7925A. Параметри захисту від випромінювання, такі як лінійний коефіцієнт ослаблення, ефективний атомний номер, шар половинного значення, довжина вільного пробігу та поперечний переріз поглинання швидких нейтронів, розраховувалися за допомогою програми Phy-X/PSD. За допомогою лінійної регресії отримано нові аналітичні рівняння, що дають значення параметрів радіаційного захисту.

Ключові слова: суперсплав, лінійний регресійний аналіз, параметри радіаційного захисту, аналітичні рівняння із залежністю від густини.

Надійшла/Received 24.08.2022